REDSHIFTED NEUTRAL HYDROGEN 21 CENTIMETER ABSORPTION TOWARD RED QUASARS

C. L. CARILLI

NRAO, P.O. Box O, Socorro, NM, 87801; ccarilli@nrao.edu

KARL M. MENTEN

Max Planck Institut für Radioastronomie, Auf dem Hugel 69, D-53121, Bonn, Germany

MARK J. REID

Smithsonian Astrophysical Observatory, 60 Garden St., Cambridge, MA, 02138

AND

M. P. RUPEN AND MIN SU YUN

NRAO, P.O. Box O, Socorro, NM, 87801

Received 1997 May 9; accepted 1997 September 15

ABSTRACT

We have searched for redshifted neutral hydrogen 21 cm absorption toward sources from the Stickel et al. "red quasar" subsample. The red quasar subsample is taken from the 1 Jy sample of flat-spectrum radio sources and is comprised of the 15 sources that are undetected on the POSS. Five of these red quasars have been searched for redshifted H I 21 cm absorption to optical depth levels of a few percent, and four show strong absorption, with neutral hydrogen column densities between 4 and 80×10^{18} $\times (T_s/f)$ cm^{-2}. This 80% success rate for the red quasars compares to the much lower success rate of only 11% for detecting H I 21 cm absorption associated with optically selected Mg II absorption line systems. The large neutral hydrogen column densities seen toward the Stickel et al. red quasars provide circumstantial evidence supporting the dust-reddening hypothesis, as opposed to an intrinsically red spectrum for the AGN emission mechanism. The lower limits to rest-frame values of A_V are between two and seven, leading to lower limits to the spin temperatures for the neutral hydrogen between 50 K and 1000 K, assuming a Galactic dust-to-gas ratio.

We consider the question of biases in optically selected samples of quasars caused by dust obscuration. Overall, the data on the red quasar subsample support the models of Fall & Pei for dust obscuration by damped Lyα absorption line systems and suggest that (1) there may be a significant, but not dominant, population of quasars missing from optically selected samples because of dust obscuration, perhaps as many as 20% at the POSS limit for an optical sample with a redshift distribution similar to the 1 Jy flat-spectrum quasar sample, and (2) optically selected samples may miss about one-half the high column density quasar absorption line systems.

The redshifted H I 21 cm absorption line detections presented herein are toward the sources 0108+388 at $z = 0.6685$, 0500+019 at $z = 0.5846$, and 1504+377 at $z = 0.6733$. No absorption is seen toward 2149+056 at $z = 0.740$ at a level below that seen for the three detections, although there is some uncertainty in this case as to the expected line redshift. In some systems, the absorbing gas is in the vicinity of the AGN, as either circumnuclear material or material in the general ISM of the AGN's host galaxy, as is probably the case for 0108+388 and 1504+377, and in other systems the absorption is by gas associated with galaxies cosmologically distributed along the line of sight to the quasar, as may be the case for 0500+019. The Westerbork Synthesis Radio Telescope spectrum of 1504+377 confirms the lack of H I 21 cm absorption associated with the narrow molecular absorption line system at $z = 0.67150$.

Subject headings: galaxies: active — galaxies: ISM — quasars: absorption lines — radio lines: galaxies

1. INTRODUCTION

Kühr et al. (1981) have compiled a complete, all-sky sample of 299 radio sources with flux densities of 1 Jy or more at 5 GHz and with flat radio spectral indices between 5 GHz and 2.7 GHz ($\alpha_5^{2.7} \geq -0.5$, where the spectral index is defined as $S_\nu \propto \nu^\alpha$). In the process of optical identification of all sources at declinations greater than $-20°$ in this sample, Stickel et al. (1996a) have found that 15 sources are undetected on the Palomar Observatory Sky Survey (POSS) plates. They designate these 1 Jy flat-spectrum radio sources with faint optical counterparts "red quasars." Subsequent deep imaging in the optical and near-IR by Stickel et al. (1996a) shows that these red quasars typically have faint, extended, galaxy-like emission in the optical with little or no evidence for a bright point source, while near IR

images reveal a dominant point source in most cases. Moreover, 13 of the 15 sources are variable in the near-IR, indicating emission from an active galactic nucleus (AGN), as opposed to a starburst. Stickel et al. (1996a) consider two physical models for the red colors of these sources, an intrinsically red spectrum for the AGN emission mechanism, perhaps caused by a high energy cut-off in the relativistic electron population (assuming the emission is synchrotron radiation; Bregman et al. 1981) and reddening of the spectrum by intervening dust.

Radio-selected quasar samples, such as the 1 Jy flat-spectrum source sample, are important because they avoid possible biases introduced in optically selected quasar samples by dust obscuration along the line of sight. Such obscuration may have a significant impact on the numbers

TABLE 1

OBSERVATIONAL PARAMETERS

Source (B1950) (1)	Date (2)	Frequency (MHz) (3)	S_v (Jy) (4)	t_{int} (hr) (5)	Bandwidth (MHz) (6)	Channels (7)	Resolution (km s^{-1}) (8)	rms (mJy beam^{-1}) (9)
0108+388......	1997 Jan 10	851.037	0.18 ± 0.02	12	2.5	127	6.9	15
0202+149......	1996 Nov 7	774.910	...	7	2.5	127	7.6	...
0500+019......	1996 Nov 12	896.398	1.6 ± 0.16	3	1.25	63	6.5	20
0500+019......	1996 Nov 27	896.350	...	8	2.5	127	6.5	11
1504+377......	1996 Nov 10	849.017	1.0 ± 0.1	12	2.5	127	6.9	14
2149+056......	1996 Dec 29	816.320	0.50 ± 0.05	11	2.5	127	7.2	16

of quasars seen at high redshift in optical samples and on the number of high column density absorption line systems seen toward optically selected quasars (Heisler & Ostriker 1988; Fall and Pei 1993; Webster et al. 1995; Shaver et al. 1996).

In this paper, we present a search for redshifted neutral hydrogen 21 cm absorption toward sources from the Stickel et al. (1996a) red quasar subsample using the new UHF system at the Westerbork Synthesis Radio Telescope (WSRT). These observations are intended to address a number of issues. First is the question of whether some AGNs have intrinsically red rather than dust-reddened emission spectra. The detection of a large column of neutral hydrogen would provide at least circumstantial evidence in favor of dust reddening (Carilli, Perlman, & Stocke 1992). Second is the question of the fraction of quasars missing from optical samples because of dust obscuration, as well as the fraction of missing high column density quasar absorption line systems. And third is to enlarge the sample of dusty, high column density absorption line systems in order to study the dense ISM in galaxies at significant look-back times.

2. OBSERVATIONS

The WSRT is in the process of a major upgrade of the receivers and correlator (Boonstra 1996). One goal of this upgrade is to provide almost continuous frequency coverage from 250 MHz to 1420 MHz. This system offers a new window for studies of redshifted neutral hydrogen using an interferometer. Interferometers offer significant advantages over single dishes when searching for faint, broad lines at low frequencies, including the natural mitigation of terrestrial interference due to fringe rotation, more accurate continuum flux density determination, and more linear spectral baselines.

We have used the UHF-high part of this system (750 MHz to 1000 MHz) to search for redshifted H I 21 cm absorption toward sources from the Stickel et al. (1996a) red quasar subsample. The redshifts used in the search are taken from Table 1 of Stickel et al., and are discussed in more detail in § 3. The H I 21 cm line is redshifted into the UHF high band of the WSRT for six of the nine sources in Table 1 of Stickel et al. (1996a) with known redshifts. Redshifted H I 21 cm absorption has already been detected against two of the six sources (0218+357 and 1504+377) using the 140 ft (43 m) telescope of the National Radio Astronomy Observatory (NRAO)[1] in Green Bank, West Virginia (Carilli, Rupen, & Yanny 1993; Carilli et al. 1997).

However, the spectrum of 1504+377 was marred by terrestrial interference, so we reobserved this source with the interferometer.

The sources observed with the WSRT are listed in column (1) of Table 1, along with observing dates in column (2). Column (3) lists the frequency for the observing band centers (corrected to a heliocentric rest frame), and column (4) lists the source-continuum flux densities at the observed frequency, as determined from off-line channels. The error bars reflect a 10% uncertainty in absolute calibration. Columns (5), (6), and (7) give the on-source integration time, total bandwidth, and number of frequency channels. Columns (8) and (9) give the velocity resolution and the root mean square (rms) noise in the final spectra. Note that all of these sources are phase calibrators for the NRAO Very Large Array, and accurate positions can be found in Taylor & Perley (1996). We use the B1950 designation for the sources, in keeping with previous papers.

Both linear polarizations were received for each of the 40 baselines connecting the 10 fixed and four moveable Westerbork antennas, although for some observations one or two of the antennas were inoperable. The data were gain-, phase-, and bandpass-calibrated using the Astronomical Image Processing System (AIPS) at the National Radio Astronomy Observatory in Socorro, New Mexico. The quasars 3C 286, 3C 48, and 3C 147 were observed for absolute flux calibration according to the scale of Baars et al. (1977) and for initial antenna-based phase calibration. Self-calibration on the target continuum sources was then employed for further refinement of the antenna-based phase solutions. The absolute gain calibration accuracy is about 10%, as estimated by applying calibration from one standard calibrator to another. Data were inspected for interference and other problems, and bad data were removed from the visibility dataset. In the case of 0202+149, strong terrestrial interference (TV channel 48) was present in the observing band close to the line frequency, precluding observation of this source by the WSRT.

The calibrated and edited data were Fourier transformed to produce images for each frequency channel, and these channel images were assembled into an image "cube." The AIPS program "IMLIN" was then used to subtract the continuum emission in the field by fitting a linear baseline to off-line channels at each pixel in the image cube. The subsequent continuum-subtracted image cubes were then deconvolved using the Clark CLEAN algorithm as implemented in the AIPS task "APCLN" (Clark 1980). In each case, the CLEANing was terminated when residual components equaled twice the rms noise per channel. The Gaussian restoring CLEAN beams for each source are listed in the figure captions. Radio spectra were then extracted at the position of the continuum source and con-

verted to optical depth using the continuum source flux density. Finally, these optical depth spectra were analyzed for integrated optical depth and velocity structure by fitting Gaussian components. All redshifts quoted have been corrected to the heliocentric reference frame. Three of the four target sources were unresolved by the WSRT, with the exception of $0108 + 388$, as discussed in § 3.1.

3. RESULTS AND ANALYSIS

3.1. $0108 + 388$

The radio source $0108 + 388$ is associated with a narrow emission line galaxy at $z = 0.670$ with $R = 22.0$ mag (Stickel et al. 1996a; Stanghellini et al. 1993). This GHz-peaked radio source has been classified as a compact symmetric object with an inverted spectrum in the nucleus and twin jets with steeper spectra extending 3 mas from the nucleus toward the northeast and southwest (Taylor, Readhead, & Pearson 1996; Conway et al. 1994). Unlike most compact symmetric objects, this source also shows large-scale structure, having a steep-spectrum jet extending about $25''$ to the east of the nucleus (Baum et al. 1990). Optical images of the field show a very red, diffuse, and slightly asymmetric galaxy, perhaps a face-on spiral, although the faintness of the galaxy makes classification difficult (Stanghellini et al. 1993). The radio source projects within $0''.5$ of the center of this galaxy. There is no evidence for a strong point-source contribution in the R-band image of $0108 + 388$. The I-band image is more compact, leading Stanghellini et al. (1993) to propose an increased contribution from the active nucleus in the near IR, perhaps indicating "the existence of nuclear obscuration" toward the AGN in $0108 + 388$. Monitoring by Stickel et al. (1996a) shows variability of this source in the near IR, with a very red observed color during IR maximum ($\alpha_{\rm IR}^{\rm opt} \leq -3$).

We have searched for H I 21 cm absorption toward $0108 + 388$ with the WSRT centered at the heliocentric redshift of the parent galaxy. The resulting spectrum at the position of the peak radio-continuum surface brightness is shown in Figure 1. The upper panel shows the observed spectrum after subtracting the peak surface brightness of 0.146 Jy beam^{-1} and after removing a linear baseline using a fit to off-line channels. The lower panel shows the spectrum converted to optical depth using the source-continuum flux density.

A strong H I 21 cm absorption line is detected at $z = 0.66847$ with a width of 100 km s^{-1} and a peak optical depth of 0.44. The continuum source is resolved with the WSRT at 851 MHz with a peak surface brightness of 146 mJy beam^{-1} and a total flux density of 180 mJy (Fig. 2, upper panel). The contours in the upper panel of Figure 2
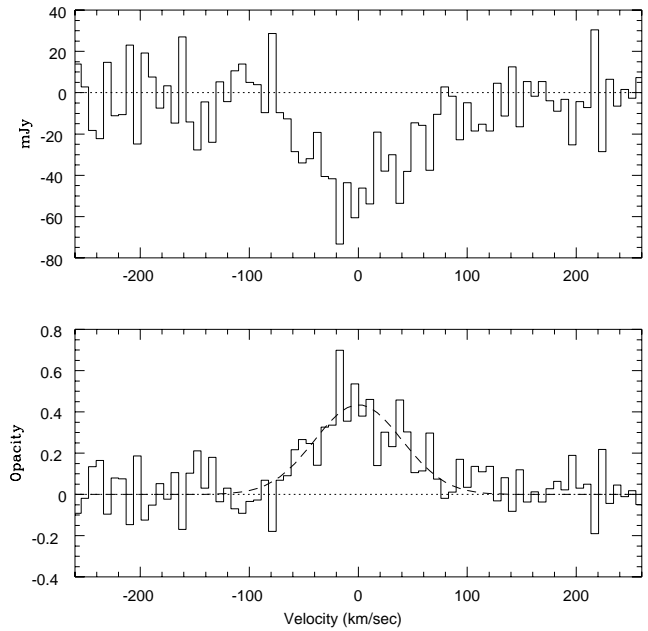

FIG. 1.—*Upper panel*: redshifted H I 21 cm absorption spectrum toward $0108 + 388$ for WSRT observations on 1996 January 10. The Gaussian restoring beam for this observation was FWHM $= 38'' \times 23''$, with the major axis oriented north to south. The zero point of the velocity scale corresponds to a heliocentric redshift of 0.66847 for the H I 21 cm line. The peak surface brightness of 0.146 Jy beam^{-1} has been subtracted and a linear baseline removed using a fit to off-line channels. *Bottom panel*: H I optical depth spectrum plus a single-component Gaussian model fit (*dashed line*). The parameters for the fit in this and subsequent figures are given in Table 2.

extend to the east, consistent with emission from the large-scale jet seen by Baum et al. (1990). The H I absorption line image shows no indication of extension of the absorption toward the east (Fig. 2, *lower panel*), although the sensitivity is such that we can set only a 1 σ limit of 0.25 to the optical depth toward the jet at a distance of $20''$ east of the nucleus (σ ≡ spectral rms noise).

The absorption profile is fitted reasonably well by a single Gaussian component (the dashed line in the lower panel of Fig. 1) whose parameters are listed in Table 2, although we cannot preclude a profile composed of a few narrower, blended components. Column (2) in Table 2 lists the heliocentric redshift corresponding to zero velocity in the spectrum (the "reference redshift" $\equiv z_{\rm ref}$), and column (3) lists the heliocentric redshift corresponding to the peak of the absorption component ($z_{\rm abs}$). Column (4) lists the component velocity relative to the reference redshift. Columns (5), (6), and (7) list the velocity integrated optical depth, the

TABLE 2
GAUSSIAN MODEL PARAMETERS

| Source	$z_{\rm ref}$	$z_{\rm abs}$	Velocity (km s^{-1})	Integrated Optical Depth (km s^{-1})	Optical Depth	FWHM (km s^{-1})	N(H I) ($\times 10^{18}$ T_s/f cm^{-2})
$0108 + 388$......	0.66847	0.66847 ± 0.00003	0 ± 4	46 ± 7	0.44 ± 0.04	94 ± 10	80.7
$0500 + 019$......	0.58457	0.58480 ± 0.00002	43 ± 3	2.5 ± 0.3	0.036 ± 0.003	62 ± 7	4.5
$0500 + 019$......	...	0.58442 ± 0.00003	-27 ± 5	1.4 ± 0.3	0.027 ± 0.003	45 ± 9	2.5
$1504 + 377$......	0.67150	0.67331 ± 0.00007	325 ± 19	7.0 ± 4.3	0.073 ± 0.045	85 ± 22	12.8
$1504 + 377$......	...	0.67324 ± 0.00001	313 ± 1	4.0 ± 0.6	0.22 ± 0.03	16 ± 2	7.3
$1504 + 377$......	...	0.67343 ± 0.00001	347 ± 1	13.4 ± 4	0.34 ± 0.08	34 ± 5	24.4
$2149 + 056$......	0.74000	0.740 ± 0.0023	...	<0.5	<0.015	29	<0.8
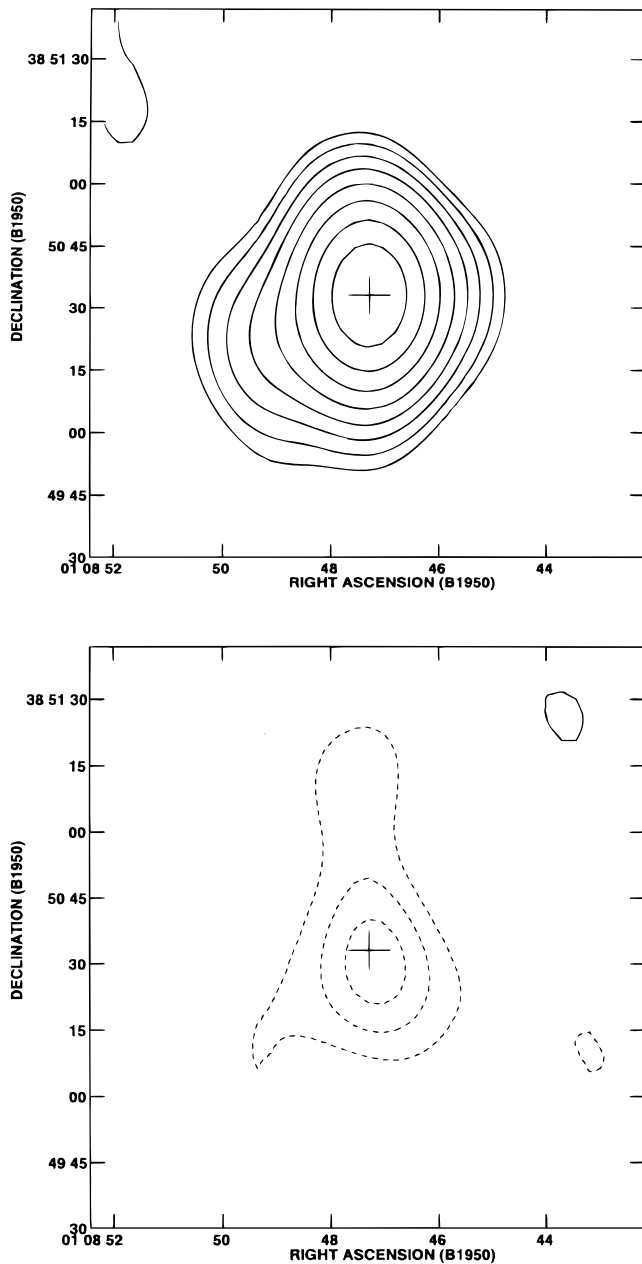
FIG. 2.—*Upper panel*: Radio-continuum image of $0108+388$ at 851 MHz with a Gaussian restoring beam of FWHM $= 38'' \times 23''$, with the major axis oriented north to south. The contours levels are -20, -14, -10, 10, 14, 20, 28, 40, 57, 80, and 113 mJy beam^{-1}, and the peak surface brightness is 146 mJy beam^{-1}. *Lower panel*: Continuum-subtracted spectral channel image for redshifted H I 21 cm absorption toward $0108+388$ at $z_{\odot} = 0.66847$, corresponding to the peak optical depth in H I with a velocity resolution of 6.9 km s^{-1}. The contour levels are -64, -48, -32, -16, 16, 32, 48, and 64 mJy beam^{-1}. Dashed contours are negative. The cross indicates the position of the peak surface brightness in the continuum image in the upper panel.

peak optical depth, and the velocity full width at half maximum (FWHM), respectively. Column (8) lists the integrated H I column density for the component. The integrated H I column density for this system is $80 \times 10^{18} \times (T_s/f)$ cm^{-2}, where T_s is the spin temperature of the gas and f is the H I covering factor.

Using the spectrum of the total radio emission from $0108+388$ and the spectrum of the core-jet emission on milliarcsecond scales (Baum et al. 1990), we estimate that the milliarcsecond scale structure in $0108+388$ contributes

about 70% of the total flux density at 851 MHz and about 85% of the peak surface brightness as seen by the WSRT at 851 MHz. Further, the compact nucleus has an inverted spectrum such that the low-frequency emission from the core-jet must be dominated by the jet (Baum et al. 1990). Given the 44% optical depth observed in the H I 21 cm line, it appears likely that the H I covers most of the milliarcsecond jet structure in $0108+388$. The implied lower limit to the cloud size is then about 6 mas, or 36 pc for $H_0 = 65$ km s^{-1} Mpc^{-1} and $q_0 = 0.5$.

We have also searched for absorption by the 2 cm $2_{11}-2_{12}$ transition of H_2CO associated with the redshifted H I 21 cm absorption system toward $0108+388$ using the Very Large Array operated by the National Radio Astronomy Observatory on 1997 June 21. This line is redshifted to 8683.692 MHz. The source-continuum flux density is 0.943 Jy at this frequency. No absorption was detected to a 1 σ limit of 0.26 mJy per channel at a velocity resolution of 6.8 km s^{-1}, implying a 1 σ optical depth limit of 0.03%. This limit is comparable to the limit found for the same molecular transition in the $z = 0.6733$ H I 21 cm absorption line system seen toward $1504+377$ (Carilli et al. 1997).

3.2. $0500+019$

The radio source $0500+019$ shows an exponential cut-off in the spectrum going from the near-IR into the optical (Stickel et al. 1996b). The source is also variable in the near-IR and in the radio (Stickel et al. 1996a), and the radio source is unresolved at cm wavelengths at resolutions ranging from a few mas to a few arcseconds (Taylor & Perley 1996; Hodges & Mutel 1984).

A 2.2 μm image of this source reveals a point source with faint emission extending $3''$ to the south, with a total magnitude of $K = 15.9$ mag. The R-band image shows an $R = 20.7$ mag inclined disk or lenticular galaxy with a major axis of about $4''$ (Stickel et al. 1996b). This galaxy is associated with a group of 10 galaxies distributed over an area of about $60''$. There is no evidence for a point source in the R-band image, although the galaxy brightness profile is asymmetric, peaking about $1''$ to the north of center along the major axis of the galaxy, coincident within the errors with the position of the K-band point source.

Optical spectra of this system reveal a moderate-ionization narrow emission-line spectrum (Stickel et al. 1996b). From four narrow emission lines, and from the Ca II H and K absorption lines, the redshift for this galaxy is found to be $z = 0.5834 \pm 0.0014$, where the error indicates the full spread in estimated redshifts for all the lines. Stickel et al. (1996b) also detect a narrow emission line at 0.6354 μm that cannot be reasonably identified with the $z = 0.5834$ galaxy. Based on this unidentified emission line, on the off-center location of the 2.2 μm point source relative to the galaxy center and on the asymmetric galaxy profile in the R-band image, Stickel et al. suggest that the quasar may be a background source at $z > 0.5834$, and that the red color of the quasar is caused by dust in the foreground galaxy.

Our first WSRT spectrum of $0500+019$ was centered at the expected frequency for H I 21 cm absorption at the redshift of the galaxy, and an absorption feature was observed at the edge of the bandpass at 896.4 MHz. We then reobserved this system, centering the bandpass on the H I 21 cm absorption feature. The resulting spectra are shown in Figure 3. The top panel shows the redshifted H I
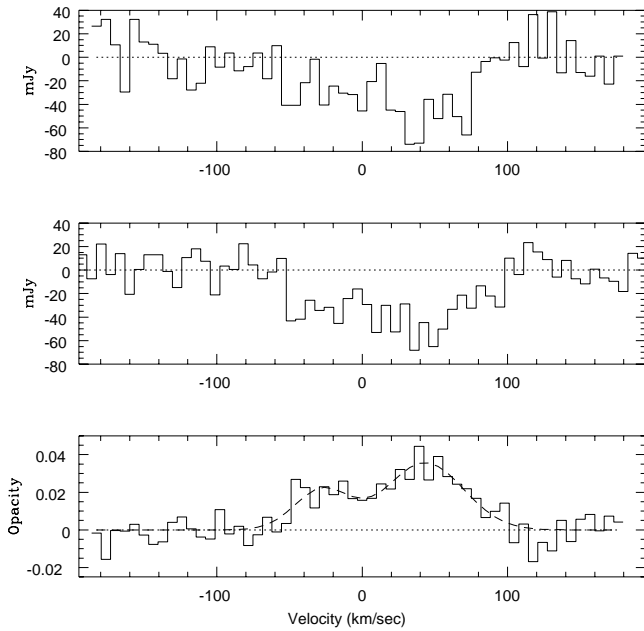
FIG. 3.—*Top panel*: redshifted H I 21 cm absorption spectrum of 0500+019 for WSRT observations on 1996 November 12. The Gaussian restoring beam for this observation was FWHM = 660″ × 23″, with the major axis oriented north to south. The zero point of the velocity scale corresponds to a heliocentric redshift of 0.58457 for the H I 21 cm line. The source-continuum flux density of 1.6 Jy has been subtracted and a linear baseline removed using a fit to off-line channels. *Middle panel*: a similar spectrum taken on 1996 November 17. *Bottom panel*: summed spectrum from the two days, weighting by integration time and converted to optical depth using the continuum flux density of the source plus a two-component Gaussian model fit (*dashed line*).

21 cm absorption spectrum for observations on 1996 November 12. The source-continuum flux density of 1.6 Jy has been subtracted, and a linear baseline has been removed using a fit to off-line channels. The middle panel shows the spectrum of 0500+019 taken on 1996 November 17. (Note that in Fig. 3 the channels for spectra from both days have been aligned such that the zero point in velocity corresponds to a heliocentric redshift of 0.58457). The bottom panel shows the summed spectrum from the two days weighted by integration time and converted to optical depth using the source-continuum flux density. The dashed line in this frame is a two-component Gaussian model fitted to the spectrum.

Broad H I 21 cm absorption is observed toward 0500+019 centered near $z = 0.58472$ and spanning about 140 km s^{-1} in velocity with a peak optical depth of about 0.04. The observed spectrum is fitted reasonably well by two Gaussian models whose parameters are listed in Table 2. The total column density (summed over both absorption components) is $6.2 \times 10^{18} \times (T_s/f)$ cm^{-2}.

3.3. *1504+377*

The flat-spectrum radio source 1504+377 (Kühr et al. 1981) is located at the center of an inclined disk, or lenticular, galaxy with a moderate-excitation narrow emission-line spectrum at $z = 0.674 \pm 0.001$ (Stickel & Kühr 1994). The parent galaxy may be associated with a group of galaxies and has a close companion galaxy at a projected distance of 4″ (Stickel & Kühr 1994). The source shows evidence for flaring of its near-IR intensity, although optical images of 1504+377 show no indication of a bright AGN (Stickel & Kühr 1994; Stickel et al. 1996a).

Recent radio spectroscopic observations of 1504+377 have revealed strong H I 21 cm absorption and absorption by a number of molecular species at the redshift of the parent galaxy (Wiklind & Combes 1996a; Carilli et al. 1997), suggesting that the very red color of this quasar is caused by extinction. In this case, evidence favors extinction by gas in the quasar's host galaxy and, in particular, by dust in a circumnuclear torus associated with the AGN itself (Wiklind & Combes 1996a; Carilli et al. 1997). The molecular absorption in this system shows two distinct velocity components, a narrow line system (line width ≤ 10 km s^{-1}) at $z = 0.67150$ and a broad line system (line width = 100 km s^{-1}) at $z = 0.6733$. The velocity separation for the two systems is 330 km s^{-1}. The H I 21 cm absorption is detected only over the velocity range covered by the broad molecular absorption line system, and the optical redshift of the galaxy corresponds to within the errors with this broad line system.

The WSRT observations of 1504+377 had two primary goals. The first goal was to verify the lack of H I 21 cm absorption at the redshift of the narrow molecular absorption system. The single dish spectrum taken with the NRAO 140 ft telescope was corrupted by terrestrial interference very close in frequency to the narrow line system. The second goal was to obtain a more accurate line profile for the broad line system, since the single dish spectrum had nonlinear spectral baselines and a 10% uncertainty in the line-to-continuum ratio caused by difficulties in determining the continuum source flux density.

The WSRT spectrum of 1504+377 is shown in Figure 4. The zero point of the velocity scale was chosen to be consistent with that of Wiklind & Combes (1996a), corresponding to the heliocentric redshift of the narrow absorption line system at $z = 0.67150$. The upper panel shows the observed spectrum after subtracting the peak surface brightness of 1.0
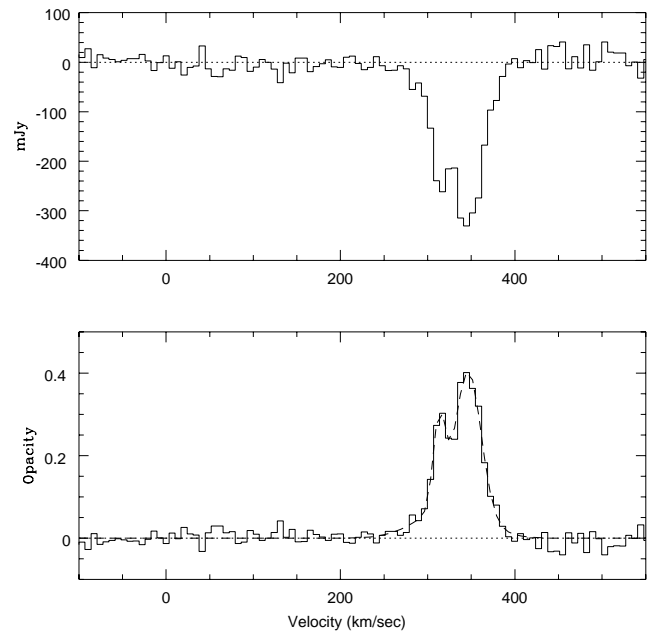

FIG. 4.—*Upper panel*: redshifted H I 21 cm absorption spectrum of 1504+377 for WSRT observations on 1996 November 10. The Gaussian restoring beam for this observation was FWHM = 39″ × 23″, with the major axis oriented north to south. The zero point of the velocity scale corresponds to a heliocentric redshift of 0.67150 for the H I 21 cm line. The source-continuum flux density of 1.0 Jy has been subtracted and a linear baseline removed using a fit to off-line channels. *Lower panel*: H I optical depth spectrum plus a three-component Gaussian model fit (*dashed line*).
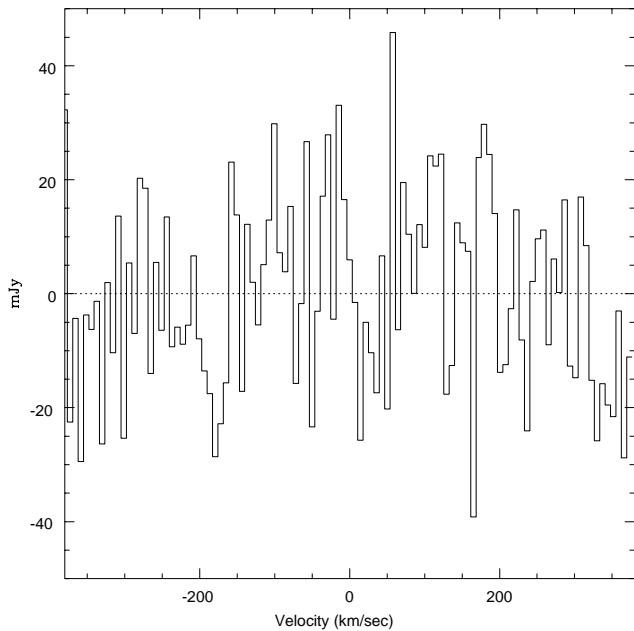
FIG. 5.—Redshifted H I 21 cm absorption spectrum toward 2149+056 for WSRT observations on 1996 December 29. The Gaussian restoring beam for this observation was FWHM = 220″ × 23″, with the major axis oriented north to south. The zero point of the velocity scale corresponds to a heliocentric redshift of 0.74000 for the H I 21 cm line. The continuum flux density of 0.50 Jy has been subtracted and a linear baseline removed using a fit to all channels.

Jy beam^{-1} and after removing a linear baseline using a fit to the off-line channel. The lower panel shows the spectrum converted to optical depth using the source-continuum flux density.

The WSRT spectrum confirms the broad absorption line system at $z = 0.6733$ and the lack of H I 21 cm absorption associated with the narrow molecular line system at $z = 0.67150$. The rms noise in the WSRT spectrum is 14 mJy at a velocity resolution of 6.9 km s^{-1}. Hence the 1 σ column density limit for H I absorption associated with the narrow molecular line system is $0.2 \times 10^{18} \times (T_s/f)$ cm^{-2}. A detailed discussion of the possible implications of the paucity of neutral hydrogen associated with this molecular cloud at $z = 0.67150$ can be found in Carilli et al. (1997).

Following Carilli et al. (1997), we have fitted a three-component Gaussian model to the broad absorption line system toward 1504+377 (see Table 2). The resulting velocities for the two high optical depth components agree to within 1 km s^{-1} with results from the 140 ft telescope. However, the opacities are about 20% higher in the WSRT spectrum. This latter difference can be attributed to the more accurate, and somewhat lower, flux density for the background source and a more linear spectral baseline in the WSRT spectrum. The integrated H I column density for the system (summed over the three absorption components) is $42 \times 10^{18} \times (T_s/f)$ cm^{-2}.

3.4. 2149+056

The 2149+056 radio source is associated with an $R = 20.4$ mag emission line galaxy at $z = 0.740$ (Stickel & Kuhr 1993). Stickel et al. (1996a) find evidence for a very steep optical spectrum and moderate variability in the near-IR. They suggest that this object is an "IR variable quasar within a luminous galaxy." The radio source is unresolved at cm wavelengths at resolutions ranging from 0″.15 to a few

arc seconds (Taylor & Perley 1996).

We searched for H I 21 cm absorption at $z = 0.740$ toward 2149+056 using the WSRT. The resulting spectrum, after subtracting the peak surface brightness of 0.50 Jy beam^{-1} and after removing a linear baseline using a fit to all the channels, is shown in Figure 5.

No absorption is seen to an optical depth limit (1 σ) of 0.03 at 7.2 km s^{-1} resolution. We have also smoothed the spectrum to lower velocity resolution and find no absorption to an optical depth limit of 0.015 at 29 km s^{-1} resolution. The corresponding column density limit is N(H I) $\leq 0.4 \times 10^{18} \times (T_s/f)$ cm^{-2} for a narrow line (7 km s^{-1}) or $0.8 \times 10^{18} \times (T_s/f)$ cm^{-2} for a broad line (29 km s^{-1}).

4. DISCUSSION

4.1. Reddening toward Red Quasars

We have searched for redshifted neutral hydrogen 21 cm absorption toward five sources from the Stickel et al. (1996a) red quasar subsample with the new UHF system at the WSRT. Three of the five show 21 cm absorption (0108+388, 0500+019, and 1504+377), while no absorption was seen toward 2149+056 at a level below that seen for the three detections. The WSRT spectra of 0202+149 were corrupted by terrestrial interference. A sixth source on the Stickel et al. red quasar list, 0218+357, had been detected previously in H I 21 cm absorption at $z = 0.6847$ (Carilli et al. 1993), and we include this source in the discussion below.

The average value of the radio-to-optical spectral index, $\alpha_{\rm rad}^{\rm opt}$, for optically identified flat-spectrum radio loud quasars is $\alpha_{\rm rad}^{\rm opt} = -0.6$ (Condon et al. 1983), while the values for the red quasar subsample are $\alpha_{\rm rad}^{\rm opt} < -0.9$. On the other hand, the radio–to–near-IR spectral indices for most of the red quasar subsample are $\alpha_{\rm rad}^{\rm IR} \geq -0.8$, implying significant steepening of the spectra between the near IR and the optical, $\alpha_{\rm IR}^{\rm opt} \ll -1$ (Stickel et al. 1996a). A rough lower limit to the required extinction can be derived by comparing the observed optical flux density with that predicted by extrapolating the radio-to-IR spectrum into the optical. This is a lower limit because of confusion by emission from stars in the galaxy with which the absorbing gas is associated. Values of the rest-frame visual extinction, A_V, range from $A_V \geq 2$ for 0108+388 and 0500+019 to $A_V \geq 3$ for 0218+357 (Menten & Reid 1996) and to $A_V \geq 7$ for 1504+377. Using the observed value of N(H I) derived from the H I 21 cm absorption lines leads to lower limits to the spin temperatures of about 50 K for 0108+388, 300 K for 1504+377, 500 K for 0500+019, and 1000 K for 0218+357, assuming a Galactic dust-to-gas ratio (Spitzer 1978) and $f = 1$.

The large neutral hydrogen columns seen toward these four red quasars provide circumstantial evidence for the reddening hypothesis, as opposed to the hypothesis of an intrinsically red spectrum for the AGN emission mechanism. While we cannot rule out the latter hypothesis based on the H I absorption data alone, the required dust-to-gas ratios would have to be less than about 0.1 to 0.3 times Galactic in order to reduce the A_V values significantly below unity for reasonable values of T_s.

Of the five red quasars from the Stickel et al. (1996a) sample that have been searched to reasonable optical depths in H I 21 cm absorption, the only source that is not

detected in absorption is 2149+056, leaving open the possibility of an intrinsically red emission spectrum for this source. However, Stickel et al. (1996a) point out that the apparent magnitude of the "parent" galaxy for 2149+056 is anomalously bright given the redshift of 0.740, and they raise the possibility that the emission line spectrum is that of the quasar, while the galaxy, and hence the reddening material, may be at a redshift of less than 0.740. Deep optical spectroscopy of the parent galaxy could test this possibility.

We have detected high column density absorption systems in four of five sources from the radio selected red quasar subsample. This detection rate is significantly higher than in optically selected samples. For instance, two independent searches for H I 21 cm absorption associated with optically selected Mg II absorption line systems resulted in two detections out of 18 systems in both studies (Briggs & Wolfe 1983; Lane, Briggs, & Smette 1998); the optical depth limits in these studies were comparable to the limits presented here.

4.2. The Statistics of Red Quasars

We now consider the question of biases in optically selected samples of quasars caused by dust obscuration, using the statistics for the 1 Jy sample of flat-spectrum radio sources and the high detection rate of H I 21 cm absorption toward red quasars. In the following section, the term "optically selected sample" means a sample of quasars selected from a moderately deep optical survey such as the POSS, with a redshift distribution comparable to that of the 1 Jy quasar sample.

The Stickel et al. (1996a) red quasar subsample was drawn from 299 flat-spectrum sources in the complete all-sky 1 Jy sample of radio sources (Kürh et al. 1981), with the additional constraint of declination greater than $-20°$. Correcting for the area of the sky covered then implies a total of about 200 sources, of which Stickel et al. find that 81.5% are quasars and 11% are galaxies. The remaining 7.5% are unidentified on the POSS (the 15 "red quasars'), implying a magnitude limit of $m \geq 20$, or $\alpha_{rad}^{opt} < -0.9$. Assuming that the 80% detection rate of H I 21 cm absorption toward the five sources discussed herein applies to the red quasar subsample as a whole leads to a lower limit of $(0.8 \times 15)/200 = 6\%$ on the fraction of quasars "missing" from an optically selected sample because of dust obscuration. An upper limit to this fraction can be estimated by making the extreme assumption that all the red quasars and galaxies in the sample are dust-obscured quasars. This leads to an upper limit of $(22+15)/200 = 20\%$ on the fraction of missing quasars.

Fall & Pei (1993) have presented detailed models of the numbers of quasars missing from optically selected samples because of obscuration by dust associated with high column density quasar absorption line systems as a function of redshift. The redshift distribution of the 1 Jy flat-spectrum quasar sample shows a broad peak at $z \approx 1$, with a tail to higher redshifts (Stickel, Meisenheimer, & Kühr 1994). Using this redshift distribution, the models of Fall & Pei predict that between 2% and 12% of the sources would be missing from such a sample because of dust obscuration.

We can also make a rough estimate of how many high column density quasar absorption line systems are missing from optically selected quasar samples. The statistics of damped Lyα systems in optically selected samples implies a redshift distribution function of the form $N(z) = 0.015 \times (1 + z)^{2.3}$, where $N(z)$ is the number of absorption systems with $N(H I) \geq 2 \times 10^{20}$ cm^{-2} per unit redshift (Rao, Turnshek, & Briggs 1995). Combining this function with the redshift distribution of the Stickel et al. quasar sample leads to an expected number of 17 high column density absorption systems toward their optically identified quasars (i.e., out of about 163 sources). Again, assuming that the 80% detection rate of H I 21 cm absorption toward the five red quasars studied herein applies to the red quasar subsample as a whole leads to a lower limit of $(0.8 \times 15)(17 + 0.8 \times 15) = 40\%$ on the fraction of high column density absorption systems missing from optically selected samples. The upper limit to this fraction is $(15+22)/(15+22+17) = 70\%$, again determined by making the extreme assumption that all the galaxies and red quasars in the Stickel et al. flat-spectrum source sample have high column density absorption systems. The comparable numbers from the models of Fall & Pei (1993) are between 30% and 60% (see also Fall & Pei 1995).

We should emphasize that there are a number of significant uncertainties in the statistics presented above. First is simply the small number of red quasars searched thus far for redshifted H I 21 cm absorption. Second are the possible biases introduced by the fact that, because of practical observational limitations, our absorption searches were limited to the specific redshifts of the parent galaxies of the absorbing clouds, as determined from emission lines seen in deep optical spectra (Stickel et al. 1996a). It is possible that we have underestimated the number of high column density systems by not searching over the full redshift range in each case (e.g., absorption systems associated with dwarf galaxies might be missed). Conversely, this selection criterion might skew the results toward absorbers at the redshift of the quasar host galaxy (see § 4.3), which perhaps could bias the statistics in the opposite sense. For instance, omitting the two associated systems in this study would reduce the detection rate of H I 21 cm absorption to $\leq 40\%$. Third is the fact that the fairly high radio flux density limit of the 1 Jy sample biases the sample toward lower redshift quasars: the redshift distribution of the 1 Jy quasar sample peaks at $z \approx 1$ while quasar samples derived from radio surveys with lower flux density limits peak at $z \approx 2$, close to the redshift peak found for optically selected quasar samples (Shaver et al. 1996; Hewitt & Burbidge 1987). While the redshift distribution is used explicitly in the calculations above, unbiased searches for redshifted H I 21 cm absorption toward a sample of red quasars selected from fainter radio catalogs would make for a fairer comparison with the optical data.

Overall, the statistics presented above should not be considered rigorous but only representative. Still, the red quasar data support the basic conclusions of Fall & Pei (1993): (1) there may be a significant, but not dominant, population of quasars missing from optically selected samples because of obscuration, perhaps as high as 20% at the POSS limit for an optical sample with a redshift distribution similar to the 1 Jy flat-spectrum quasar sample; and (2) optically selected samples may miss about one-half of the high column density quasar absorption line systems. A final point made by Fall & Pei is that the strongest bias in optical samples may be against the high column density systems with high metallicities and high dust-to-gas ratios. Such systems might be the most interesting from the perspective of follow-up radio studies of the dense, pre–star

forming ISM in galaxies at significant look-back times. The data presented herein suggests that searching for redshifted H I 21 cm absorption toward red quasars may be an effective method for circumventing this bias.

4.3. *The Location of the Absorbing Material*

In some sources in our study, the absorption and presumably the reddening are caused by material in the quasar's host galaxy, as appears to be the case for 1504+377 at $z = 0.673$ (Carilli et al. 1997; Wiklind & Combes 1996a) and for 0108+388 at $z = 0.6685$. In 1504+377 and 0108+377, the velocity widths for the absorption systems are large (≈ 100 km s^{-1}) and, hence, are comparable to line widths seen for systems associated with nearby Seyfert galaxies and other low-redshift AGNs (Dickey 1983; van Gorkom et al. 1989; Conway & Blanco 1995). High-resolution imaging of the absorption toward a number of nearby AGNs indicates that the high velocity-dispersion gas is local to the AGNs, perhaps in a circumnuclear torus or ring with size scale of order 10 pc, and that the velocity width reflects the torus dynamics (Israel et al. 1991; Gallimore et al. 1994; Mundell et al. 1995a, 1995b; Conway 1997).

In other red quasars, the absorption is caused by material in galaxies cosmologically distributed along the line of sight to the quasar. One such intervening system is the gravitational lens 0218+357, the smallest "Einstein ring" radio source, for which H I 21 cm and molecular absorption has been detected toward the radio source at $z = 0.687$ (Carilli et al. 1993; Wiklind & Combes 1995; Menten & Reid 1996). In retrospect, gravitational lensing may not be surprising for such systems, since one requires a low impact parameter line of sight in order to intercept the denser regions of the ISM of the intervening galaxy. An important conclusion is that at least some gravitational lenses are gas-rich systems, as has also been found in the case of the Einstein ring radio source PKS 1830−211 (Wiklind & Combes 1996b; Frye, Welch, & Broadhurst 1997; Menten, Carilli, & Reid 1998).

The case for a cosmologically intervening absorption system versus an associated system for 0500+019 is unclear (see § 3.2). A possible argument against the intervening hypothesis for 0500+019 is the broad H I 21 cm absorption line profile (total velocity width 140 km s^{-1}). This is much larger than the 10–20 km s^{-1} velocity dispersion expected for a line of sight perpendicular to the disk of a spiral galaxy (Dickey & Lockman 1990) and might argue for absorption by circumnuclear gas, as discussed above. An additional puzzle for this system is that the H I redshift is offset from the optical redshift by $+240 \pm 265$ km s^{-1} (i.e., infalling relative to the optical galaxy), although the uncertainty in the optical redshift is large. If the absorber is an intervening system, a possible model to explain both the large velocity offset and the large velocity dispersion may be galactic rotation, in the case where the quasar projects off-center along the major axis of a highly inclined disk galaxy. For example, if the galaxy rotation velocity was 200 km s^{-1} and the line of sight to the quasar cut through the edge-on disk halfway out along the major axis, the expected line width due to differential rotation would be about 100 km s^{-1}. One possible difficulty with this model is that H I 21 cm absorption seen through the disk of the Milky Way Galaxy typically appears as a series of discrete narrow components with widths of a few km s^{-1} (Dickey et al. 1983). Unfortunately, the sensitivity of the current WSRT spectrum of 0500+019 is insufficient to differentiate between a blend of narrow components and two broad shallow lines.

REFERENCES

Baars, J., Genzel, R., Pauliny-Toth, I., & Witzel, A. 1977, A&A, 61, 99
Baum, S. A., O'Dea, C. P., Murphy, D. W., & de Bruyn, A. G. 1990, A&A, 232, 19
Bregman, J. N., Lebofsky, M. J., Aller, M., Reike, G. H., Aller, H., Hodge, P., Glassgold, A., & Huggins, P. 1981, Nature, 293, 714
Briggs, F. H., & Wolfe, A. M. 1983, ApJ, 268, 76
Boonstra, A.-J. 1996, NFRA Newsl., 11, 4
Carilli, C. L., Menten, K. M., Reid, M. J., & Rupen, M. P. 1997, ApJ, 474, L89
Carilli, C. L., Perlman, E. S., & Stocke, J. T. 1992, ApJ, 400, L13
Carilli, C. L., Rupen, M. J., & Yanny, B. 1993, ApJ, 412, L59
Clark, B. G. 1980, A&A, 89, 377
Condon, J. J., Condon, M. A., Broderick, J. J., & Davis, M. M. 1983, AJ, 88, 20
Conway, J. E. 1997, in IAU Colloq. 164, Radio Emission from Galactic and Extragalactic Compact Radio Sources, ed. J. A. Zensus, J. Wrobel, & G. B. Taylor (Berkeley: PASP), in press
Conway, J. E., & Blanco, P. R. 1995, ApJ, 499, L131
Conway, J. E., Myers, S. T., Pearson, T. J., Readhead, A. C., Unwin, S. C., & Xu, W. 1994, ApJ 425, 568
Dickey, J. M. 1983, ApJ, 263, 87
Dickey, J. M., Kulkarni, S. R., Heiles, C. E., & van Gorkom, J. H. 1983, ApJS, 53, 591
Dickey, J. M., & Lockman, F. J. 1990, ARA&A, 28, 215
Fall, S. M., & Pei, Y. C. 1993, ApJ, 402, 479
———. 1995, in QSO Absorption Lines, ed. G. Meylan (Heidelberg: Springer), 23
Frye, B., Welch, W. J., & Broadhurst, T. 1997, ApJ, 478, L25
Gallimore, J. F., Baum, S. A., Odea, C. P., Brinks, E., & Pedlar, A. 1994, ApJ, 422, L13
Heisler, J., & Ostriker, J. 1988, ApJ, 332, 543
Hewitt, A., & Burbidge, G. 1987, ApJS, 63, 1
Hodges, M. W., & Mutel, R. L. 1984, AJ, 89, 1391

Israel, F. P., van Dishoeck, E. F., Baas, F., Koornneef, J., Black, J., & de Graauw, T. 1990, A&A, 227, 342
Kühr, H., Witzel, A., Pauliny-Toth, I. I., & Nauber, U. 1981, A&AS, 45, 367
Lane, W., Briggs, F. H., & Smette, A. 1998, in Probing the Intergalactic Medium with Quasar Absorption Lines, ed. P. Petitjean, in press
Menten, K. M., Carilli, C. L., & Reid, M. J. 1998, in preparation
Menten, K. M., & Reid, M. J. 1996, ApJ, 465, L99
Mundell, C. G., Pedlar, A., Axon, D. J., Meaburn, J., & Unger, S. W. 1995a, MNRAS, 277, 641
Mundell, C. G., Pedlar, A., Edlar, A., Baum, S. A., Odea, C. P., Gallimore, J. F., & Brinks, E. 1995b, MNRAS, 272, 355
Rao, S., Turnshek, D., & Briggs, F. H. 1995, ApJ, 449, 488
Shaver, P. A., Wall, J. V., Kellermann, K. I., Jackson, C. A., & Hawkins, M. R. S. 1996, Nature, 384, 439
Spitzer, L., Jr. 1978, Physical Processes in the Interstellar Medium (New York: Wiley)
Stanghellini, C., O'Dea, C. P., Baum, S. A., & Laurikainen, E. 1993, ApJS, 88, 1
Stickel, M., & Kühr, H. 1994, A&AS, 105, 67
Stickel, M., Meisenheimer, K., & Kühr, H. 1994, A&AS, 105, 211
Stickel, M., Rieke, G. H., Kühr, H., & Rieke, M. J. 1996a, ApJ, 468, 556
Stickel, M., Rieke, M. J., Rieke, G. H, & Kühr, H. 1996b, A&A, 306, 49
Taylor, G. B., & Perley, R. A. 1996, VLA Calibration Manuel (Socorro: NRAO)
Taylor, G. B., Readhead, A. C., & Pearson, T. J. 1996, ApJ, 463, 95
van Gorkom, J. H., Knapp, J. H., Ekers, R. D., Ekers, D. D., Laing, R. A., & Polk, K. S. 1989, AJ, 97, 708
Webster, R. L., Francis, P. J., Peterson, B. A., Drinkwater, M. J., & Masci, F. J. 1995, Nature, 375, 469
Wiklind, T., & Combes, F. 1995, A&A, 299, 382
———. 1996a, A&A, 315, 86
———. 1996b, Nature, 379, 139